

**H. Mazhar<sup>1</sup>, C.Y. Ching<sup>2</sup>**

<sup>1</sup> Canadian Nuclear Laboratories, Chalk River, Ontario, Canada  
(hazem.mazhar@cnl.ca)

<sup>2</sup> McMaster University, Hamilton, Ontario, Canada  
(chingcy@mcmaster.ca)

## **Effect of Flow Conditions on Flow Accelerated Corrosion in Pipe Bends**

### **Abstract**

Flow Accelerated Corrosion (FAC) in piping systems is a safety and reliability problem in the nuclear industry. In this study, the pipe wall thinning rates and development of surface roughness in pipe bends are compared for single phase and two phase annular flow conditions. The FAC rates were measured using the dissolution of test sections cast from gypsum in water with a Schmidt number of 1280. The change in location and levels of maximum FAC under single phase and two phase flow conditions are examined. The comparison of the relative roughness indicates a higher effect for the surface roughness in single phase flow than in two phase flow.

### **1. Introduction**

Piping degradation is a serious concern in nuclear power generation facilities. A great portion of this degradation is caused by Flow Accelerated Corrosion. Pipe wall thinning due to FAC occurs by: (i) chemical oxidation of the pipe base material followed by, (ii) the mass transfer of the oxide porous layer into the flowing medium exposing the pipe to additional oxidation. The mass transfer of the oxide layer depends primarily on the flow dynamics of the adjacent fluid and the flow conditions, such as single or two phase flow [1].

The current study is focused on FAC in 90° bends since it is one of the most common failure modes [1]. The severe changes in flow direction resulting in flow separation and redistribution into two phase flow [2] [3] and a high turbulence level [4] contribute to high levels of FAC. Several studies were focused on the flow dynamics and pressure drop in bends under single and two phase flows. Flow circulation near the inlet to a bend with flow acceleration on the inner wall side was reported under different single phase flow conditions [5] [6]. The flow continues to accelerate into the bend with high velocity shifting off the inner wall toward the outer wall, where elevated flow velocities have been observed near the bend outlet. Similar flow features were observed under two phase flow conditions, especially at low void fraction (ratio of gas to liquid in the cross section) [7]. The intensity of FAC is reported to increase as the void fraction increases [7]. Under annular two phase flow, the focus of the current study, the flow approaches the bend with a liquid annulus surrounding a gas core (air in the current study). The flow accelerates near the bend inlet; with liquid separation from the inner wall depositing on the latter parts of the outer wall near the bend outlet [8]. In addition, entrained liquid droplets in the gas core would impinge on the outer wall of the bend and thus enhance FAC.

The effect of surface roughness on mass transfer enhancement was investigated in several studies [9]-[13]. A hydrodynamic fully rough surface was reported to enhance heat and mass transfer by approximately 3 to 4 times over a smooth surface for single phase flow. The surface roughness effect was considered to be more dominant than the pipe geometry for the mass transfer enhancement. The effect of surface roughness on mass transfer under liquid-gas two phase flow was studied for a range of relative roughness [14]. A larger effect of relative roughness on mass transfer enhancement is reported for two phase bubbly flow than in single phase flow. The range of Reynolds number considered were below 18000, which indicates that a fully rough surface was not reached for the tested conditions. Poulson [16] reported a visually smooth surface topology under annular two phase flow in U-shape pipe bends. The development and effect of the surface roughness on mass transfer under two phase flow, in particular for high void fraction, is not clear.

The current study compares the features and mechanisms of FAC between single and annular two phase flow using test sections cast from Gypsum with a density of  $1580 \text{ kg/m}^3$ , which has been reported previously [9]-[11]. The Schmidt number ( $Sc$ ), which controls the mass transfer rate and thus FAC is 1280. This is comparable to the dissolution of the oxide layer of carbon steel components in water. Surface roughness develops due to mass transfer to the bulk flow and thus mimics the development of the surface topology experienced in nuclear power plant piping [9] [12]. The technique is very useful since the surface roughness plays a significant role in determining the mass transfer rate and overcomes the limitation of using heat transfer correlations to determine mass transfer with surface roughness evolution.

## **2. Experimental Facility and Methodology**

The experiments were performed in a 2.54 cm diameter single and two phase (air/water) flow loop shown schematically in Figure 1 [10] [11]. The water is circulated from a 100 litre reservoir using a centrifugal pump. The water flow is regulated via a globe valve and measured using turbine flow meters with an accuracy of  $\pm 1\%$  of the flow reading. Air flows from a compressed line and supplied to the test facility. The air flow rate is measured using two rotameters in parallel with accuracies of  $\pm 2\%$  of the full scale. The air pressure is monitored and recorded to correct the rotameter readings and determine the actual air flow rates. A mixing chamber in the form of two concentric tubes with a perforated inner tube, carries the air. The air is injected into the water stream running in the annulus between the inner and outer tubes to generate the two phase flow.

The water or mixed air–water flow then passes through a straight pipe of 160 cm in length upstream of the test section. The air-water flow exits the test section to a 75 cm long straight pipe before being directed to a phase separation reservoir with an air vent to release the separated air. The two phase flow conditions were located on a two phase flow map [12] in the annular flow zone, using air/water superficial velocities and confirmed with flow visualization in the upstream transparent pipe.

The water temperature was measured in the reservoir and kept constant to within  $\pm 0.5^\circ\text{C}$  using a compensation cooling loop. The dissolution of the Gypsum test section in water during the test increases the water electrical conductivity which is used to determine the overall dissolved mass from the test section in the water. The water reservoir included an electrical conductivity probe to measure the water conductivity. A calibration experiment was performed offline to correlate the amount of dissolved Gypsum to the change in conductivity of the water.

The gypsum test sections are cast with a nominal diameter of 2.54 cm and consisted of an upstream 20 cm long straight pipe, a standard 90° bend with a radius of curvature of 38.1 cm, and followed by a 10 cm long downstream straight section. The cast sections are left to dry and their weight is recorded periodically. When the weight becomes steady, the sections are tested under single and annular two phase flow conditions. After each experiment the test sections are allowed to dry again and when the samples weights are constant, the difference in samples weights before and after experiments is taken as a measure of the overall mass removed. The test sections are then cut along the bend profile, Figure 2, to measure the surface topography using a laser scanning coordinate measurement technique to obtain the wear rates. The total mass removed from the test section during the experiment was determined from: (i) comparing the mass of the test section before and after the test, (ii) the concentration of the dissolved gypsum in the water at the end of each test, and (iii) the integrated mass removed obtained from the laser digitized three dimensional surface scan. The calculated mass removed from the different methods agreed to within  $\pm 7\%$ .

The mass transfer coefficient is evaluated from:

$$\rho \frac{d\delta}{dt} = h\Delta C \quad (1)$$

where  $\rho$  is the average density of the Gypsum,  $\delta$  is the thickness of local mass removed normal to the surface,  $\Delta C$  is the difference between species concentration at the wall and in the bulk flow and  $h$  is the mass transfer coefficient. The concentration difference decreases over the course of the experimental time due to the dissolution of the gypsum in water, and thus the driving potential for the mass transfer decreases. The mass transfer coefficient was calculated using a modified time to account for the change in concentration in the bulk flow using the following:

$$\rho \frac{d\delta}{d\tau_{\text{mod}}} = h\Delta C_o \quad (2)$$

where  $\tau_{\text{mod}}$  is the modified time given by:

$$\tau_{\text{mod}} = \frac{1}{\Delta C_o} \int_0^t [C_w - C_b] \cdot dt \quad (3)$$

Then the Sherwood number is calculated as:

$$Sh = \frac{h \times D}{D_m} \quad (4)$$

where  $D$  is the pipe diameter and  $D_m$  is the mass diffusivity. The rate of change in the wear is computed to determine the spatial distribution of the mass transfer rate. The uncertainty in the measurements was evaluated considering all the contributing variables, e.g., uncertainty in the digitized image, water electrical conductivity, variability from different testing times [10]. The uncertainty in the local mass transfer coefficient was determined to be approximately  $\pm 15\%$  in the two phase experiments and  $\pm 18\%$  in the single phase case.

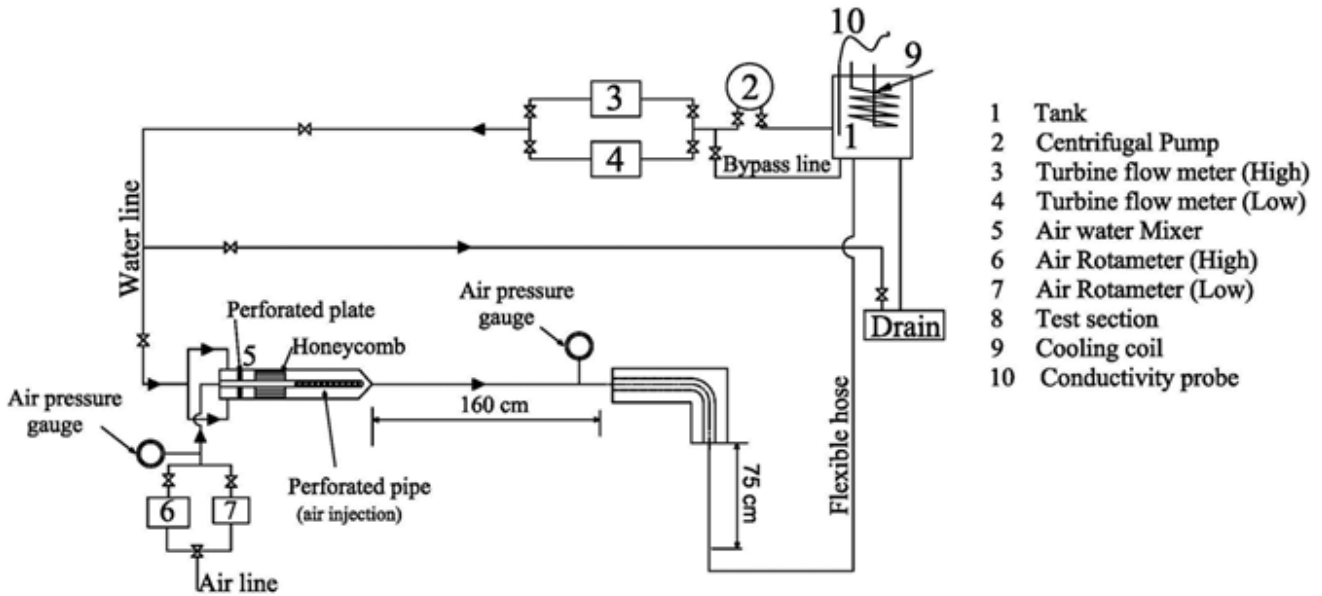


Figure 1 Schematic of the test facility showing the main components of the flow loop

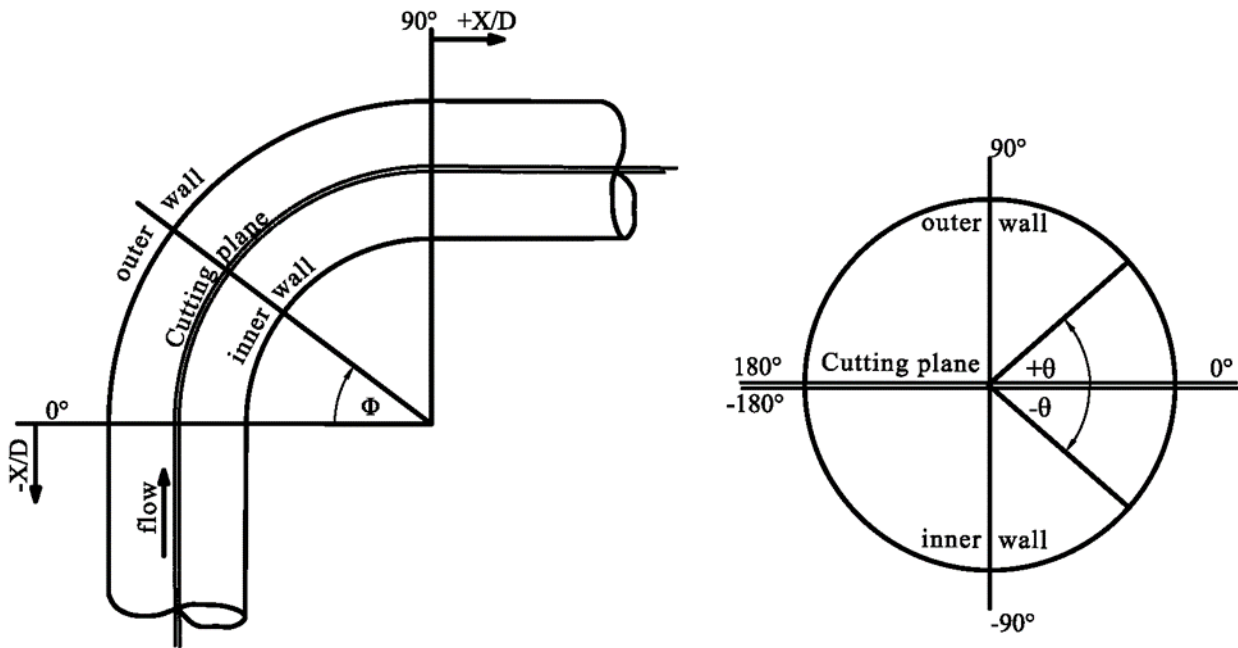


Figure 2 Schematic of the test section showing the section planes relative to: (a) streamwise orientation, and (b) crosswise orientation

Since the mass transfer in two phase flow systems could result from dissolution and/or erosion, the contribution of the two processes was evaluated by performing experiments with different initial gypsum bulk concentrations of 0%, 50% and fully saturated in the water. The fully saturated experiments

resulted in no mass removal while the mass transfer coefficients from the other two initial concentrations were within the experimental uncertainty. This indicates that mass transfer for the current experimental conditions is purely by dissolution.

### **3. Results and Discussion**

#### **3.1 Mass Transfer Distribution**

The typical mass transfer distributions in a single 90° bend under single phase flow for a Reynolds number of 70,000 and annular two phase flow at liquid and gas superficial velocities of 0.28 m/s and 29 m/s respectively, based on several experiments [10] [11], are shown in Figure 3. In the single phase case, a high mass transfer region was observed on the bend inner wall on both sides of the symmetry line and the mass transfer levels decayed along the bend curvature, in the flow direction, with the high mass transfer regions shifting along the side walls toward the outer wall. A low mass transfer region was observed on the bend inner wall near the exit while a significant increase was observed on the bend outer wall as the flow exits the bend. In the annular two phase flow case, the mass transfer was uniform at the entrance to the bend inner wall and decreases into the bend with no observed mass transfer enhancement on the side walls.

Images of the worn surface topology under single and two phase flows are shown in Figure 4. The mass transfer in the different regions was accompanied by surface streaks and traces that correspond to flow features at the different locations as explained in [10]. The low mass transfer observed near the outlet of the bend inner wall was distinguished with a smooth surface topology which corresponds to flow separation zone and flow turbulence. In the annular flow case the surface topology was mostly smooth except at the areas of high mass transfer enhancement where a deep valley with few isolated pits was observed. The peak region in this case was distinguished with small pits due to impingement of suspended droplets and liquid streaks.

Three regions of elevated mass transfer were identified in the single phase experiments: (i) near the inlet to the bend inner wall in the form of two localized cells around the symmetry plane, (ii) on the sidewalls midway into the bend curvature in the form of tiger strips inclined to the symmetry plane, and (iii) near the outlet of the bend outer wall in the form of a large region extending beyond the bend exit. The maximum mass transfer enhancement was observed near the bend outer wall, likely corresponding to locations of maximum flow velocity as the accelerating core flow shifts toward the bend outer wall near the exit. Two locations of mass transfer enhancement were determined in the case of annular flow: (i) on the bend outer wall, midway into the bend curvature, and (ii) on the bend outer wall near the exit. The counter rotating vortices in the gas core would drive the liquid film towards the bend inner wall, resulting in a thinning of the liquid film on the bend outer wall. Meanwhile, the liquid film on the inner wall would separate due to inertia and deposit on the outer wall towards the exit of the bend.

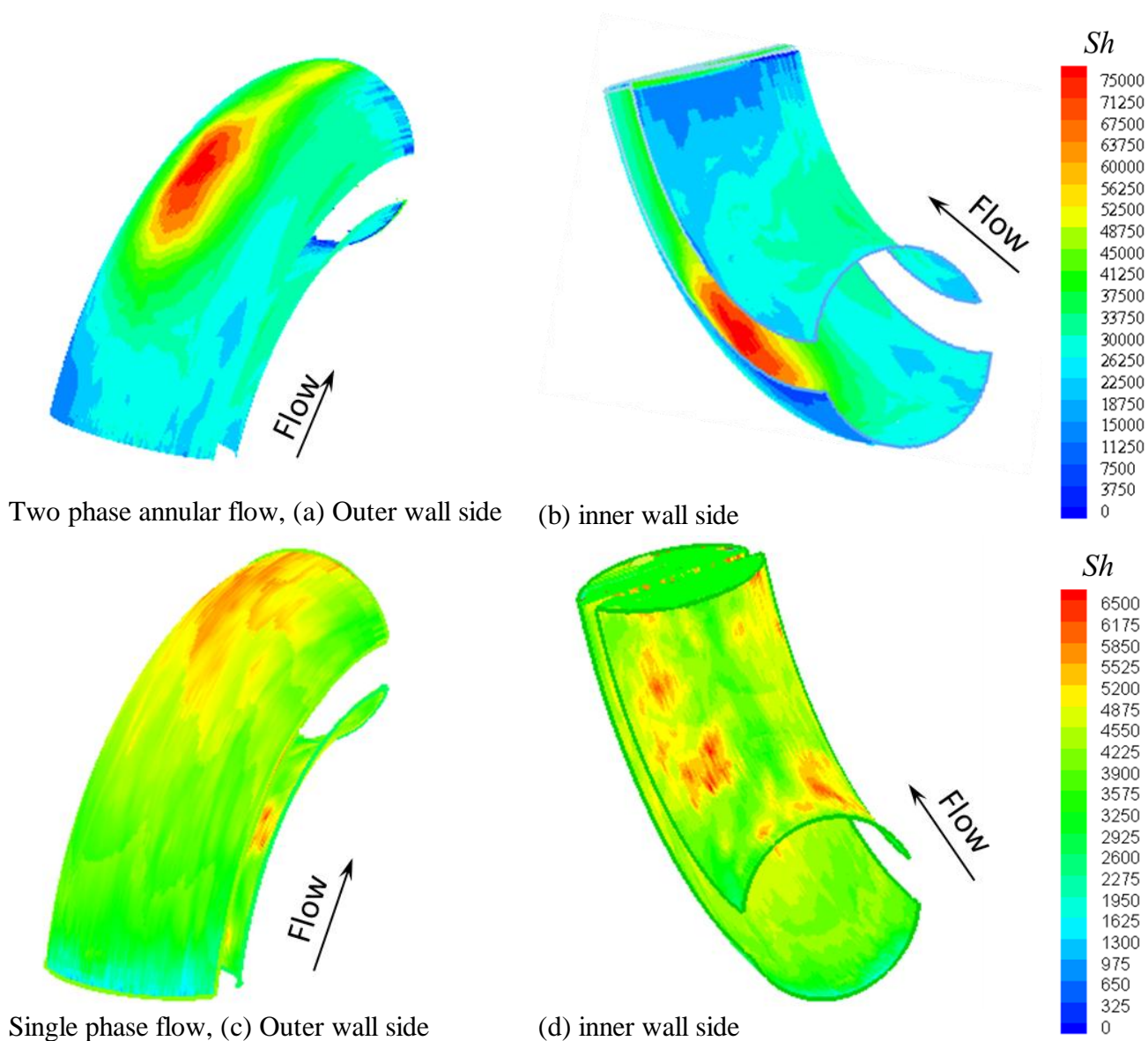


**Figure 3 Comparison of Sherwood number distribution in single bends for single and two phase annular flow**

A schematic illustrating the flow redistribution under annular two phase flow based on flow visualizations and literature is presented in Figure 5. The areas of elevated mass transfer enhancement in single phase flow is mostly correlated to regions of high flow velocity in the vicinity of the pipe wall while in two phase flow it is correlated to regions of liquid film disturbance in the near wall region due to deposition of liquid droplets separating from the inner wall side.

The relative surface roughness that develops from the single and annular two phase flow experiments is shown in Figure 6. The relative roughness is evaluated from the undulations of the surface around the local average surface pattern. The peak to valley of the undulations normalized by the diameter is used to determine the value of the relative roughness  $e/D$  [11]. In the case of single phase flow, the surface

roughness is present in the form of streaks in the direction of local flow. The streaks are in different directions at the different locations: (i) longitudinal scallops parallel to the centreline on the inner wall inlet, (ii) inclined toward the centreline on the inner side walls, and (iii) straight streaks parallel to the centre line again on the bend outer wall outlet. Smooth surface features with low roughness were observed midway into the bend inner wall between  $\phi$  of  $-25^\circ$  and  $25^\circ$  in the crosswise direction. In the two phase flow case, the roughness was concentrated near the high mass transfer region, midway into the bend outer wall, with minimal roughness on the rest of the bend inner and outer walls. The roughness appeared in the form of isolated sparse pits in random directions.

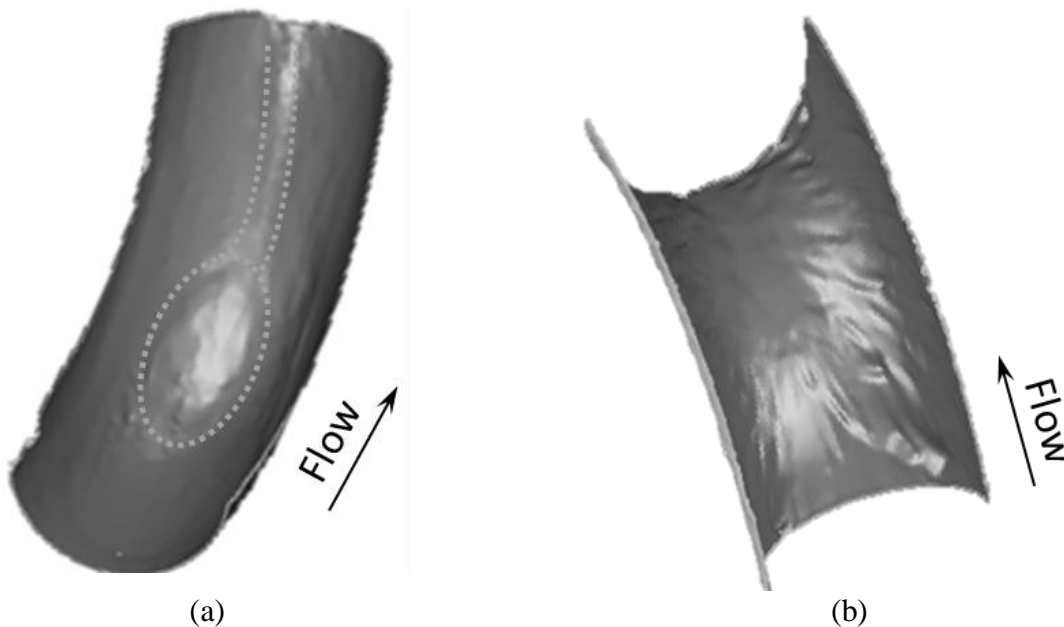
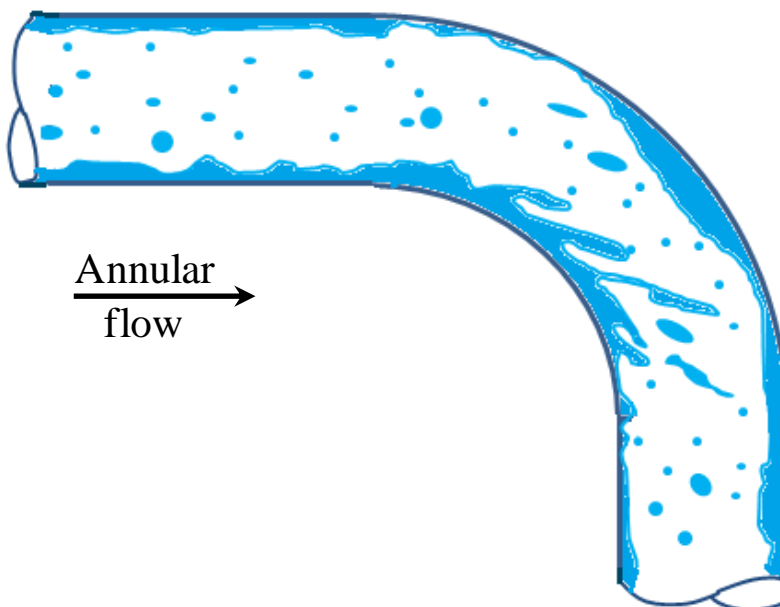


Figure 4 Dominant surface topology in a typical mass transfer experiment in: (a) Two phase, and (b) Single phase



**Figure 5 Schematic of the flow redistribution in an annular two phase flow in 90° bend**

### 3.2 Comparison of mass transfer in upstream straight pipe

The Sherwood number (Sh) in the upstream straight pipe of the tested sections for a range of annular two phase flow conditions was compared to that of single phase flow at similar average liquid flow velocity and Reynolds number. A typical straight pipe correlation was used to determine the single phase mass transfer coefficient [19]. The mass transfer coefficient was determined at the same average liquid velocity as the estimated annular liquid film velocity, similar to [20], assuming only liquid exists in the pipe cross section. The Reynolds number for the annular two phase flow was based on the pipe diameter since the mass transfer occur only on the interface between the liquid and the pipe wall.

$$Re_{single\ phase} = \frac{\rho v D_{pipe}}{\mu} \quad \text{and} \quad Re_{two\ phase} = \frac{\rho v_{film} D_{pipe}}{\mu}$$

The single phase experimental results showed a good agreement with the correlation. The comparison shows approximately 30-50% increase in Sh for the two phase flow compared to the single phase flow as shown in Figure 7. This increase could be attributed to the effect of the liquid film waviness in addition to the process of liquid droplet deposition and re-entrainment to and from the liquid film. The latter may result in penetration of the liquid viscous sublayer which could affect the mass transfer rate from the wall. The effect of roughness was also examined by comparing typical surface roughness in single and annular two phase flow as shown in Figure 8. The surface roughness in the two phase flow case appears as scattered pits over the surface with a non-distinct pattern. In the case of single phase flow, the resulting surface roughness is uniform over the entire surface. The roughness level is observed to be higher in the case of single phase flow. The mass transfer in the two phase flow is likely enhanced by an additional mechanism in addition to the surface roughness, which is possibly the disturbance caused by continuous phase redistribution.

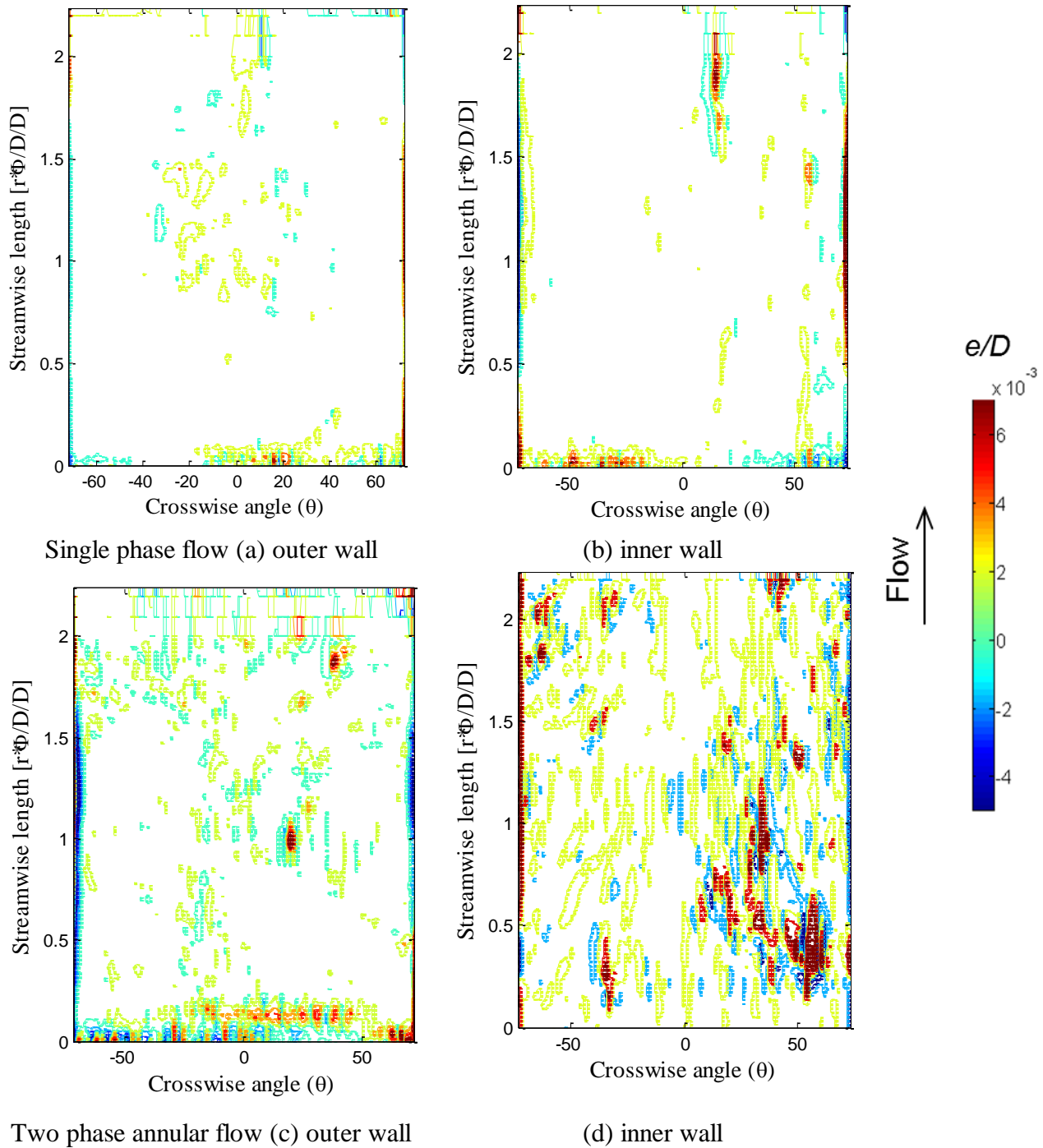


Figure 6 Comparison of the relative surface roughness in single bends under single and two phase flow

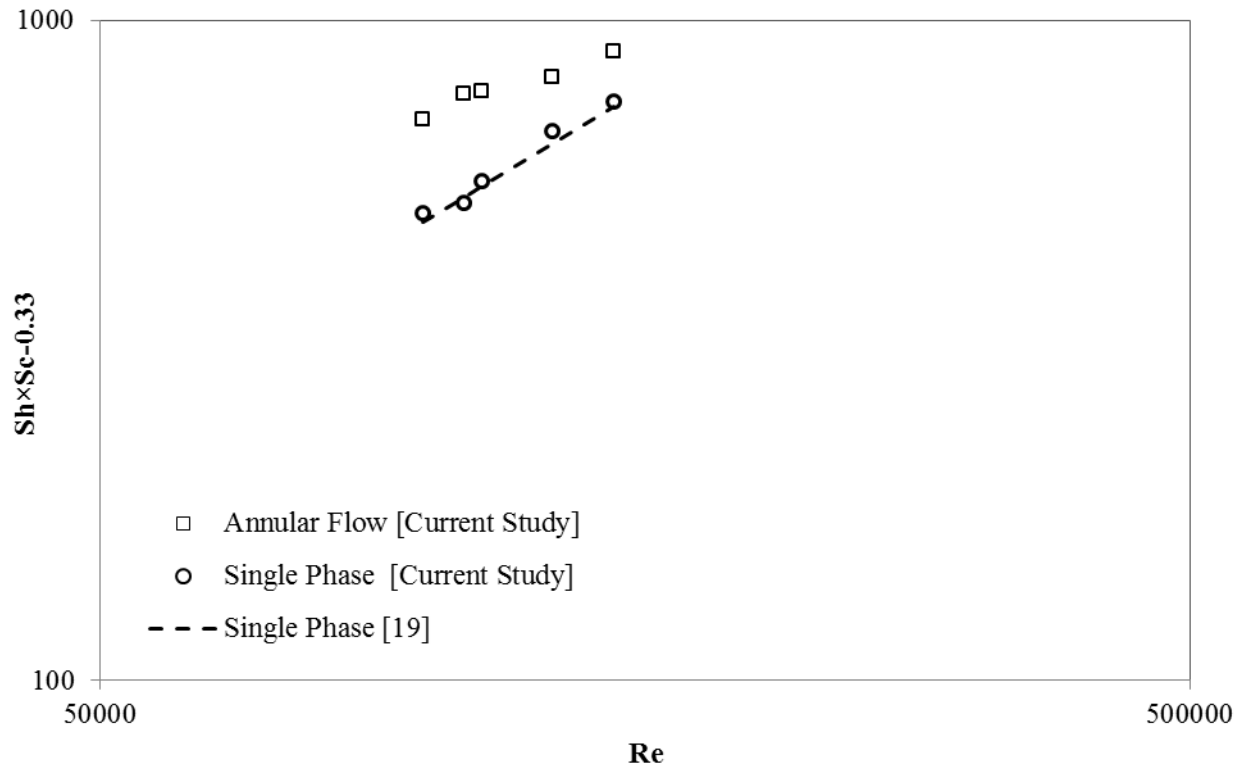


Figure 7 Comparison of the mass transfer coefficient for single and two phase flow in a straight pipe

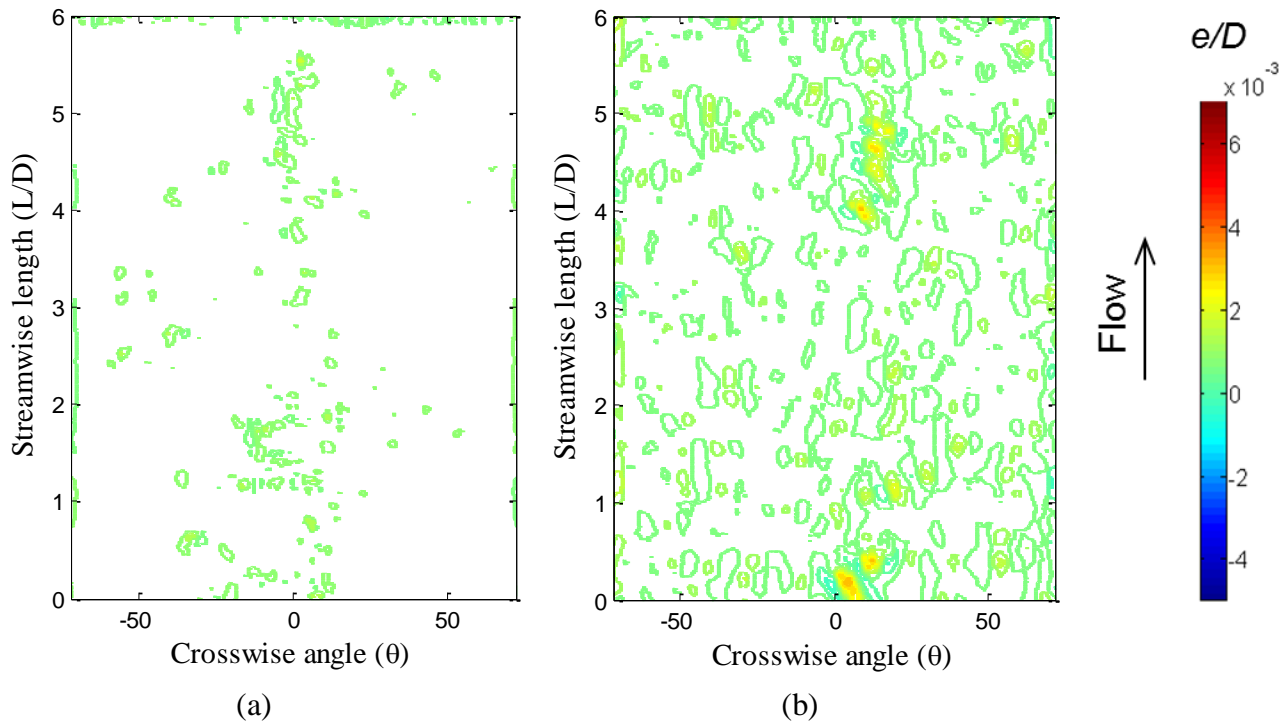


Figure 8 Comparison of the relative surface roughness in straight pipe for (a) Single phase and (b) Two phase annular flow

#### 4. Conclusion

The surface wear topology accompanying the FAC process differs significantly from single to two phase flow. Comet-like scallops were observed in the single phase case with the tails pointing in the local flow direction. Isolated scallops with no traces were observed in the case of two phase flow. Three regions of high mass transfer/FAC rates were observed in the single phase case while two high mass transfer regions were measured in the two phase annular flow case. The mass transfer enhancement is mostly driven by flow acceleration and circulation in the single phase flow, while it is coincident with the liquid deposition region in the case of two phase flow where high turbulent flow is anticipated. The mass transfer in straight pipes under annular two phase flow is approximately 30 to 50 % higher than in single phase flow for similar average liquid velocity. This could be due to the continuous liquid deposition and re-entrainment which causes a high disturbance in the liquid film on the pipe wall in the two phase flow case. High surface roughness corresponds to high mass transfer regions in single phase flow. The contribution of surface roughness to the mass transfer enhancement in two phase flow is unclear and requires further study such as the measurement of the shear stress to fully explain the mass transfer trends in single and two phase flow.

#### Acknowledgments

The support of CANDU Owners Group (COG), Atomic Energy of Canada (AECL) and the Natural Sciences and Engineering Research Council of Canada (NSERC) is gratefully acknowledged.

#### Nomenclature

$dm/dt$	Mass transfer rate	$[kg/s]$
$C_w$	Gypsum ions concentration at the wall	$[kg/m^3]$
$C_b$	Gypsum ions concentration at the bulk fluid	$[kg/m^3]$
$\Delta C_o$	Initial concentration difference	$[kg/m^3]$
$\delta$	Local instantaneous wear of the test section	$[m]$
$D$	Bend cross-sectional diameter	$[m]$
$D_m$	Mass Diffusivity for gypsum in water at 25°C	$[m^2/s]$
$h$	Mass transfer coefficient	$[m/s]$
$Sc$	Schmidt number $(\nu/D_m)$	
$Sh$	Sherwood number $(h \times D/D_m)$	
$X/D$	Streamwise dimensionless distance	
$\rho$	Density of the gypsum	$[kg/m^3]$

$\theta$	<i>Bend cross sectional angle</i>	
$\phi$	<i>Bend angle of curvature</i>	
$\nu$	<i>Kinematic viscosity</i>	$[m^2/s]$

## 5. References

- [1] R.B. Dooley, Flow Accelerated Corrosion in fossil and combined cycle/HRSG plants, Power Plant Chemistry, Vol. 10 (2), 2008
- [2] N.M., Crawford, G. Cunningham and P.L. Spedding, Prediction of pressure drop for turbulent fluid flow in 90 degree bends, Proceeding Institute of Mechanical Engineering, 217E, 1–3, 1974
- [3] S. Kim, J.H. Park, G. Kojasoy, J.M. Kelly and S.O. Marshall, Geometric effects of 90-degree elbow in the development of interfacial structures in horizontal bubbly flow, Nuclear Engineering and Design (237): 2105-2113, 2007
- [4] B. Poulson, The Local Enhancement of Mass Transfer at 180 Degree Bend, International Journal of Heat Mass Transfer, Vol. 31, No. 6, p. 1289-1297, 1988
- [5] J.R. Weske, Experimental Investigation of Velocity Distribution Downstream of a Single Duct Bend, N.A.C.A, TN-1471, 1948
- [6] E.M. Sparrow and G.M. Chrysler, Turbulent Flow and Heat Transfer in Bends of Circular Cross Section: i-Heat transfer experiments, ASME Journal of Heat Transfer, Vol. 108, p. 40-47, 1986
- [7] N. Pecherkin and V. Chekhovich, Mass Transfer in Two-Phase Gas-Liquid Flow in a Tube and in Channels of Complex Configuration, Chapter 8, Mass transfer in multiphase systems and its applications, Vol. 155, 2011
- [8] C.L. Maddock, P.M.C. Lacy and M.A. Patrick, The structure of two phase flow in a curved pipe, Journal of Chemical Engineering Symposium 38, 1-22, 1974
- [9] J. Postlethwaite and U. Lotz, Mass transfer at erosion–corrosion roughened surfaces, Canadian Journal Chemical Engineering, pp. 66–75, 1988
- [10] B. Poulson, Mass transfer from rough surfaces, Corrosion Science 30, No. 6/7: 743-746, 1990
- [11] H. Mazhar, D. Ewing, J.S. Cotton and C.Y. Ching, Experimental Investigation of Mass Transfer in 90 Degree Pipe Bends using a Dissolvable Wall Technique, International Journal of Heat and Mass Transfer, 65, p. 280–288, 2013
- [12] H. Mazhar, D. Ewing, J.S. Cotton and C.Y. Ching, Mass Transfer in Single Bends Under Annular Two Phase Flow Conditions, Journal of Heat Transfer, 136, p. 43001, 2014

- [13] T. Le, D. Ewing, C. Schefski and C.Y. Ching, “Mass transfer in Back to Back Elbows arranged in an out of Plane configuration”, International Conference on Flow Accelerated Corrosion, No. 1166, FAC 2103, 2013 May
- [14] W. Ahmed, M.M. Bello, E. Meamer and A. Al-Sarkhi, “Flow and mass transfer downstream of an orifice under flow accelerated corrosion conditions”, Nuclear Engineering and Design 252, 52 -67, 2012
- [15] G.H. Sedahmed, I.S. Mansour and G. Abd El-latif, Mass transfer controlled corrosion of pipelines under two phase(gas-liquid) flow, Vol. 29, No. 2, p. 147-151, 1994
- [16] B. Poulson, “Measuring and modeling mass transfer at bends in annular two-phase flow”, Chemical Engineering Science, Vol. 46, pp. 1069-1082, 1991
- [17] B. Poulson and R. Robinson, The local enhancement of mass transfer at 180° bends”, Intenational Journal of Heat and Mass transfer, No. 31: 1289-1297, 1988
- [18] W. Ahmed, M.M. Bello, A. Al-Sarkhi, M. El Nakla and H.M. Badr, Experimental Investigation of Flow Accelerated Corrosion under Two-phase Flow Conditions, Nuclear Engineering and Design, Vol. 267, p. 34-43, 2014
- [19] P.N. Blumberg, A study of stable, Periodic Dissolution Profiles Resulting from The Interaction of the Soluble Surface and an Adjacent Turbulent Flow, The University of Michigan, PhD, Engineering, Chemical, 1970
- [20] H. Wang, T. Hong, J. Cai and W. Jepson, Enhanced mass transfer and wall shear stress in multiphase slug flow, Corrosion 02501, 2002